

# Spatial and temporal variability of Sea Surface Temperature (SST) and Chlorophyll (Chl-a) in the coast of Ireland

G.Casal

Marine Institute, Oranmore, Galway, Ireland  
gema.casal@marine.ie

Page | 1

## Analysis of SST temporal trends

In this study, a period of 34 years (January 1982 to December 2015) of SST at monthly resolution was used to analyse the trends of the defined study area as well as for each ICES Divisions surrounding the country. As time series observations measured sequentially in time, seasonal effects especially annual cycles, are often present in the data caused directly or indirectly by the Earth's movement around the Sun. The main features of many time series are trends and seasonal variations that can be modelled deterministically with mathematical functions of time. But, another important feature of most time series is that observations close together in time tend to be correlated (serially dependent) (Copertwait and Metcalfe, 2009). Weatherhead et al., (1998) proposed a method which encompasses both the natural variability of signal and the possible existence of serial correlations between observations. This approach for the detection of trends has been broadly applied to detect trends in environmental data (e.g. Zhang and Reid, 2010; Henson et al., 2013), but to date only two studies were found to assess changes in satellite SST (Good et al., 2007; Chollett et al., 2012). Trends were calculated in this study using generalized least squares (package 'nlme' R software) by fitting the model proposed by Weatherhead et al., (1998):

$$SST_t = \mu + S_t + \frac{\omega t}{12} + N_t \quad \text{Eq. (1)}$$

where  $SST_t$  corresponds to the monthly mean averaged for the whole study area and for each ICES Division depending on the case,  $\omega$  is the linear trend of rate °C/year, and  $\mu$  is the offset at the start of the time series (for example, the offset of the monthly mean SST at January 1982),  $S_t$  corresponds to the seasonal component and is described by:

$$S_t = \sum_{j=1}^4 \beta_{1,j} \sin \frac{2\pi jt}{12} + \beta_{2,j} \cos \frac{2\pi jt}{12} \quad \text{Eq. (2)}$$

On the other hand,  $N_t$  corresponds to the monthly mean noise that is not represented by the linear trend model. It is assumed autoregressive of order 1 (AR-1 autocorrelation form) and is described by:

$$N_t = \phi N_{t-1} + \varepsilon_t \quad \text{Eq. (3)}$$

where  $\phi$  is the first-order autocorrelation and  $\varepsilon_t$  are independent and identically normally distributed random errors with a mean of zero and constant variance. The variability of  $\varepsilon_t$  (standard deviation  $\sigma_\varepsilon$ ) together with the autocorrelation parameter  $\phi$  and the number of years of data,  $n$ , was used to calculate the error of the trend estimate ( $\sigma_\omega$ ):

$$\sigma_\omega = \frac{\sigma_\varepsilon}{(1-\phi)n^{3/2}} \quad \text{Eq. (4)}$$

This implies that the precision of the trend is a function of the magnitude of the unexplained variability in the data, the autocorrelation of the noise, and the length of the time series (Weatherhead et al., 1998). The number of years of data,  $n^*$ , required to distinguish a trend from natural variability using Eq.(1) was calculated by the method of Weatherhead et al., (1998), with a probability of detection of 90% and a confidence level of 95 % :

$$n^* = \left[ \frac{3.3\sigma_\varepsilon}{|\omega|} \sqrt{\frac{1+\phi}{1-\phi}} \right]^{2/3}$$

Eq. (5)

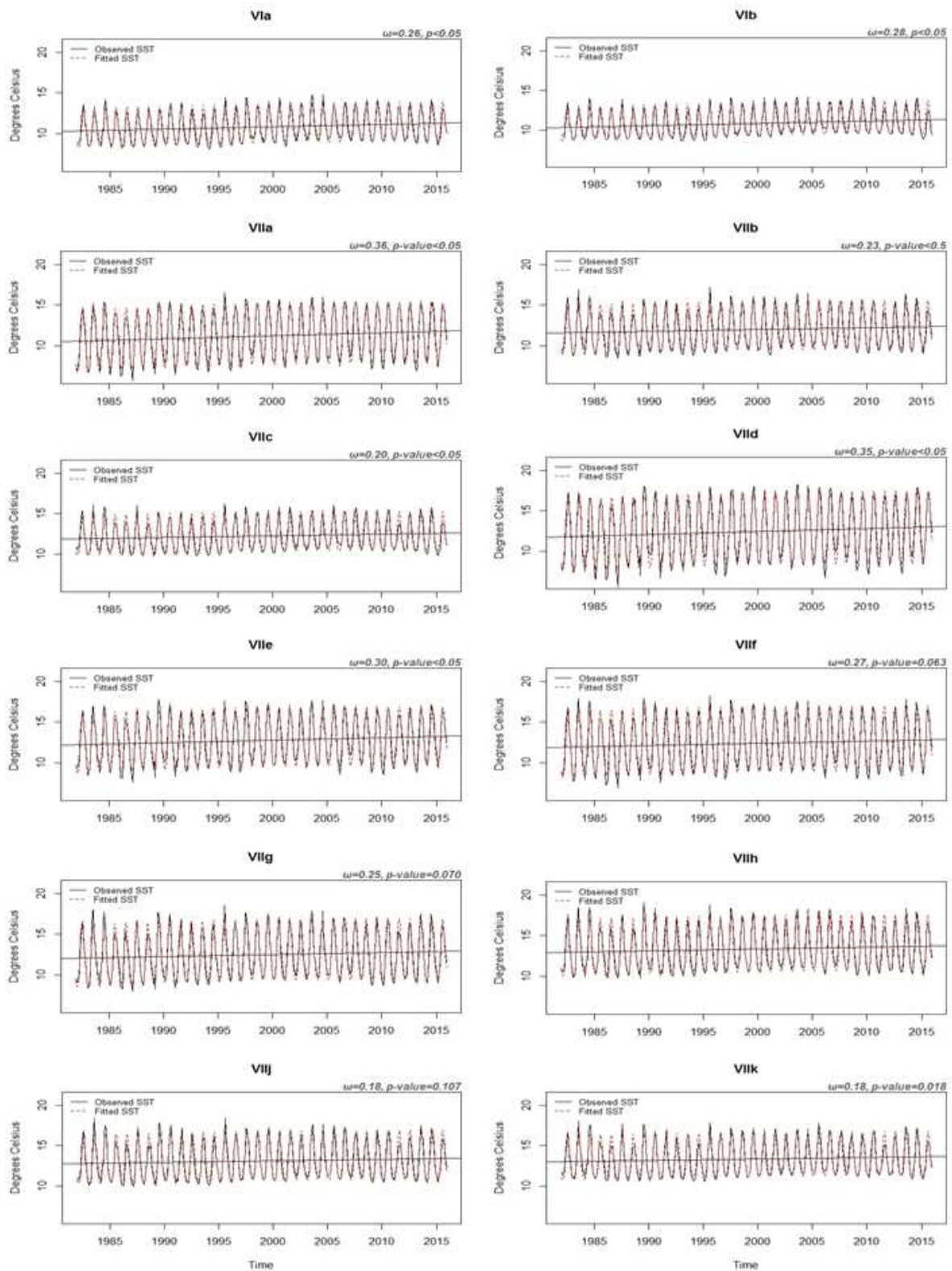


Figure 1 Observed SST (solid black line), model fitted (dashed red line) and linear trend ( $\omega$ ) in  $^{\circ}\text{C decade}^{-1}$  for each ICES Division

**Table 1. Values of the model parameters that best allow the model to reproduce the monthly data for the whole study area as well as for each of the ICES Divisions. The units of the trend ( $\omega$ ) are in  $^{\circ}\text{C year}^{-1}$ . The significant trends are represented in bold.**

Parameter	Study area		VIa		VIb		VIa		VIb		VIc		VIId	
	Value	p-value	Value	p-value	Value	p-value	Value	p-value	Value	p-value	Value	p-value	Value	p-value
$\mu$	12.3342	$\leq 0.05$	10.895	$\leq 0.05$	10.911	$\leq 0.05$	11.376	$\leq 0.05$	12.055	$\leq 0.05$	12.303	$\leq 0.05$	12.515	$\leq 0.05$
$\omega$	<b>0.026</b>	$\leq 0.05$	<b>0.028</b>	$\leq 0.05$	<b>0.030</b>	$\leq 0.05$	<b>0.036</b>	$\leq 0.05$	<b>0.023</b>	$\leq 0.05$	<b>0.020</b>	$\leq 0.05$	<b>0.035</b>	$\leq 0.05$
$\beta_{1,1}$	-40.688	$\leq 0.05$	-33.405	$\leq 0.05$	-26.736	$\leq 0.05$	-48.183	$\leq 0.05$	-29.367	$\leq 0.05$	-27.312	$\leq 0.05$	-44.391	$\leq 0.05$
$\beta_{2,1}$	-50.434	$\leq 0.05$	-42.189	$\leq 0.05$	-37.387	$\leq 0.05$	-50.647	$\leq 0.05$	-43.699	$\leq 0.05$	-35.981	$\leq 0.05$	-43.672	$\leq 0.05$
$\beta_{1,2}$	10.508	$\leq 0.05$	11.342	$\leq 0.05$	16.483	$\leq 0.05$	2.982	$\leq 0.05$	8.285	$\leq 0.05$	12.573	$\leq 0.05$	5.917	$\leq 0.05$
$\beta_{2,2}$	9.344	$\leq 0.05$	11.119	$\leq 0.05$	11.846	$\leq 0.05$	4.691	$\leq 0.05$	9.332	$\leq 0.05$	7.871	$\leq 0.05$	-0.353	0.724
$\beta_{1,3}$	-1.708	0.089	-3.850	$\leq 0.05$	-5.225	$\leq 0.05$	-0.379	0.705	-1.194	0.233	-2.440	0.015	-0.723	0.470
$\beta_{2,3}$	-1.444	0.150	-2.046	0.041	-0.744	0.457	-0.847	0.398	-0.729	0.466	-0.645	0.519	0.047	0.963
$\beta_{1,4}$	0.826	0.409	1.149	0.251	0.853	0.394	1.089	0.277	0.361	0.719	-0.358	0.721	1.708	0.088
$\beta_{2,4}$	0.272	0.786	-1.441	0.150	-1.918	0.056	0.293	0.770	-0.343	0.732	-0.298	0.766	0.239	0.811
$\phi$	0.514	0.514	0.565		0.639		0.474		0.518		0.586		0.533	
$\sigma_{\epsilon}$	0.419	0.419	0.347		0.328		0.482		0.480		0.416		0.612	
$\sigma_{\omega}$	0.004		0.004		0.005		0.005		0.005		0.005		0.007	
$n^*$	22.898		20.630		21.616		19.129		27.662		30.382		24.656	

Parameter	VIe		VIIf		VIIg		VIIf		VIIf		VIIf	
	Value	p-value	Value	p-value	Value	p-value	Value	p-value	Value	p-value	Value	p-value
$\mu$	12.8444	$\leq 0.05$	12.485	$\leq 0.05$	12.598	$\leq 0.05$	13.424	$\leq 0.05$	13.202	$\leq 0.05$	13.404	$\leq 0.05$
$\omega$	<b>0.030</b>	$\leq 0.05$	0.027	0.063	0.025	0.070	0.021	0.091	0.018	0.107	0.018	0.081
$\beta_{1,1}$	-41.883	$\leq 0.05$	-39.549	$\leq 0.05$	-33.528	$\leq 0.05$	-32.807	$\leq 0.05$	-29.831	$\leq 0.05$	-29.148	$\leq 0.05$
$\beta_{2,1}$	-45.193	$\leq 0.05$	-51.054	$\leq 0.05$	-47.236	$\leq 0.05$	-43.894	$\leq 0.05$	-41.075	$\leq 0.05$	-37.003	$\leq 0.05$
$\beta_{1,2}$	6.313	$\leq 0.05$	6.327	$\leq 0.05$	7.415	$\leq 0.05$	12.251	$\leq 0.05$	11.517	$\leq 0.05$	12.796	$\leq 0.05$
$\beta_{2,2}$	7.376	$\leq 0.05$	8.368	$\leq 0.05$	11.483	$\leq 0.05$	12.040	$\leq 0.05$	9.485	$\leq 0.05$	7.035	$\leq 0.05$
$\beta_{1,3}$	-1.550	0.122	-0.980	0.327	-0.252	0.801	-1.225	0.221	-0.864	0.388	-1.903	0.058
$\beta_{2,3}$	-2.563	0.011	-2.160	0.031	-1.533	0.126	-1.213	0.226	-1.381	0.168	-1.186	0.236
$\beta_{1,4}$	1.639	0.102	1.454	0.147	0.421	0.674	0.234	0.815	-0.047	0.962	-0.329	0.742
$\beta_{2,4}$	0.828	0.408	0.982	0.327	0.648	0.517	0.875	0.382	0.764	0.445	0.410	0.682
$\phi$	0.476		0.472		0.453		0.488		0.520		0.556	
$\sigma_{\epsilon}$	0.517		0.551		0.575		0.533		0.498		0.467	
$\sigma_{\omega}$	0.005		0.005		0.005		0.005		0.005		0.005	
$n^*$	22.923		25.066		26.872		29.591		32.862		33.644	

**Table 2 Relation of SST and NAO, AMO and EAP indices (ONI index  $\omega = -0.10$ , p-value=0.043) for the study area as well as for each ICES Divisions**

ICES Division	NAO		AMO		EAP	
	$\omega$	p-value	$\omega$	p-value	$\omega$	p-value
study area	-0.453	$\leq 0.001$	3.770	$\leq 0.001$	0.036	0.757
Vla	-0.356	$\leq 0.001$	3.027	$\leq 0.001$	0.056	0.515
VIb	-0.346	$\leq 0.001$	2.954	$\leq 0.001$	0.038	0.620
VIIa	-0.538	$\leq 0.001$	4.281	$\leq 0.001$	0.087	0.530
VIIb	-0.445	$\leq 0.001$	3.645	$\leq 0.001$	-0.003	0.979
VIIc	-0.382	$\leq 0.001$	3.036	$\leq 0.001$	-0.026	0.774
VIIId	-0.587	$\leq 0.001$	4.580	$\leq 0.001$	0.161	0.333
VIIe	-0.463	$\leq 0.001$	3.966	$\leq 0.001$	0.082	0.538
VIIIf	-0.463	$\leq 0.001$	4.363	$\leq 0.001$	0.062	0.675
VIIg	-0.534	$\leq 0.001$	3.966	$\leq 0.001$	0.005	0.973
VIIh	-0.508	$\leq 0.001$	4.041	$\leq 0.001$	0.035	0.781
VIIj	-0.457	$\leq 0.001$	3.645	$\leq 0.001$	-0.020	0.859
VIIk	-0.413	$\leq 0.001$	3.359	$\leq 0.001$	-0.042	0.679

## Analysis of Chl-a spatio- temporal variability

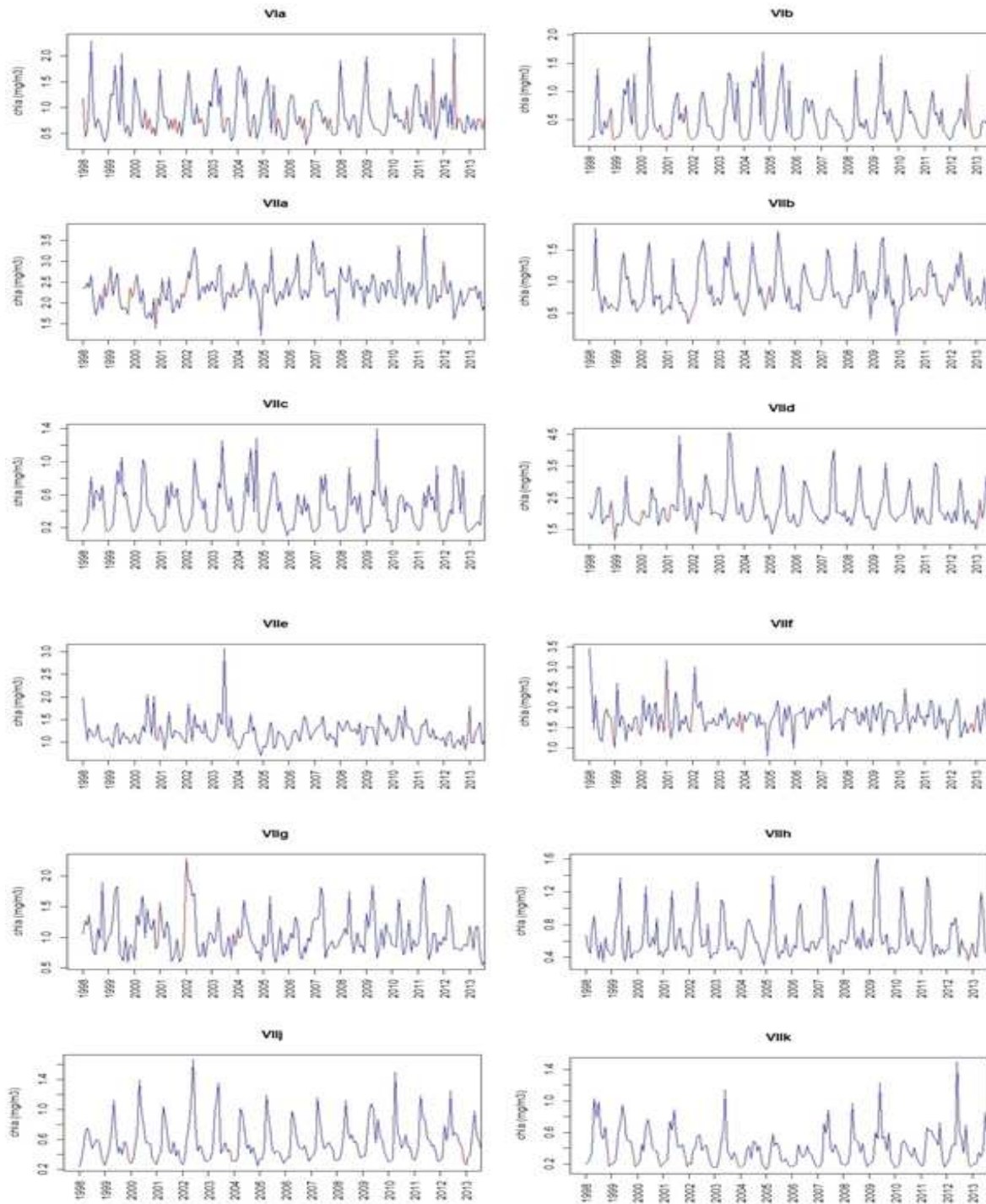


Figure 2 Time series plots for Chl-a concentration in the ICES Divisions considered

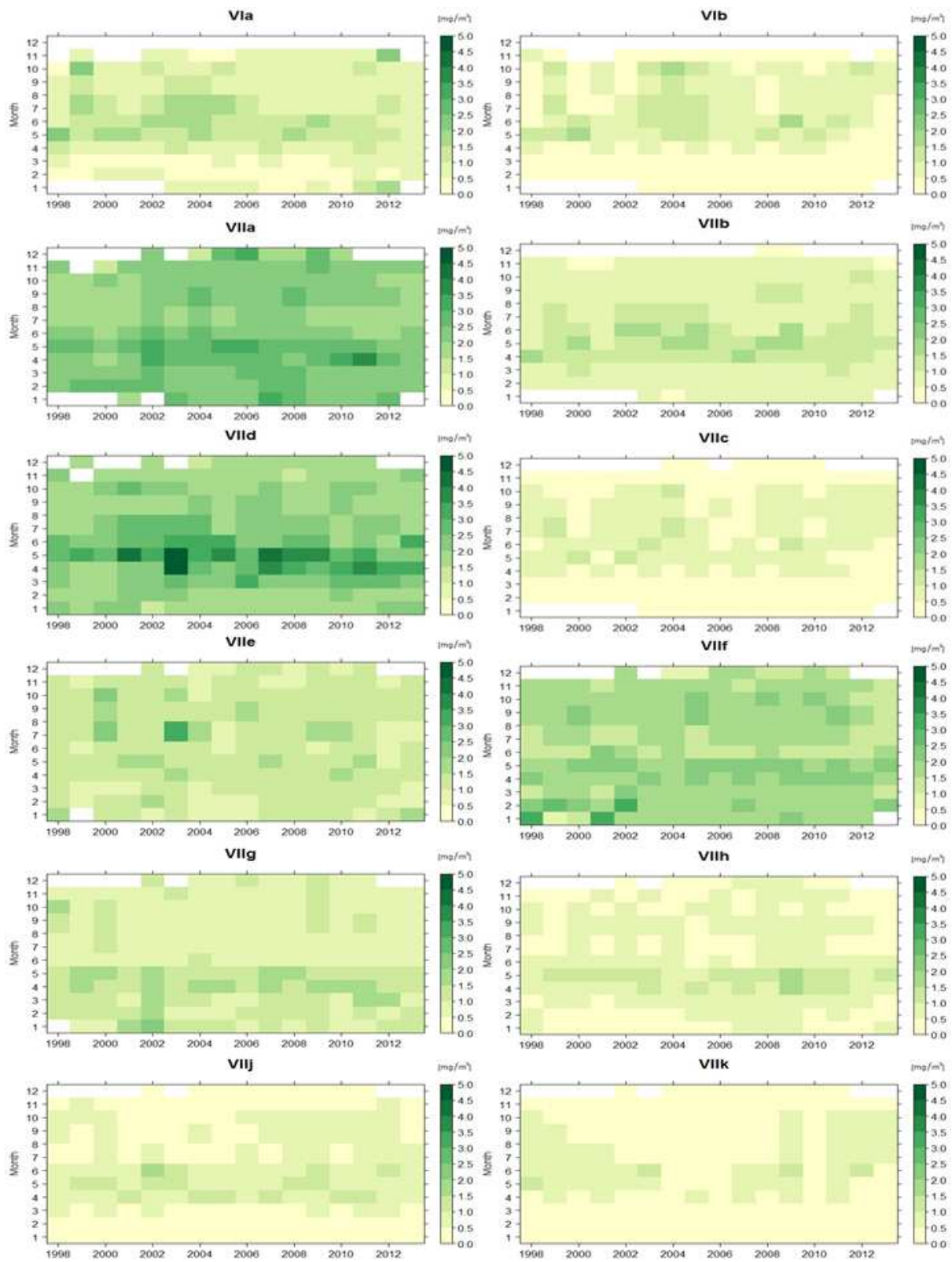


Figure 3 Levelplots representing the temporal variation of Chl-a in each ICES Division

For more information regarding this poster please refer to the ESA  
Special Publication Proceedings